

# Atrial electrical and structural abnormalities in an ovine model of chronic blood pressure elevation after prenatal corticosteroid exposure: implications for development of atrial fibrillation

Peter M. Kistler<sup>1</sup>, Prashanthan Sanders<sup>1</sup>, Miodrag Dodic<sup>2</sup>, Steven J. Spence<sup>1</sup>, Chrishan S. Samuel<sup>2</sup>, ChongXin Zhao<sup>2</sup>, Jennifer A. Charles<sup>3</sup>, Glenn A. Edwards<sup>3</sup>, and Jonathan M. Kalman<sup>1\*</sup>

<sup>1</sup>Department of Cardiology, Royal Melbourne Hospital, Melbourne 3050, Australia; <sup>2</sup>Howard Florey Institute, The University of Melbourne, Melbourne, Australia; and <sup>3</sup>Department of Veterinary Science, The University of Melbourne, Melbourne, Australia

Received 24 March 2006; revised 24 September 2006; accepted 19 October 2006; online publish-ahead-of-print 10 November 2006

See page 2919 for the editorial comment on this article (doi:10.1093/eurheartj/ehl374)

## KEYWORDS

Hypertension;  
Atrium;  
Atrial fibrillation;  
Apoptosis

**Aims** Elevated blood pressure (EBP) is the most prevalent and potentially modifiable risk factor for AF, yet little is known of its atrial effects. We aimed to characterize the atrial electrical and structural changes in a chronic ovine model of EBP after prenatal corticosteroid exposure.

**Methods and results** Twelve sheep with chronically EBP (mean arterial pressure  $94 \pm 3$  mmHg) and six controls ( $71 \pm 4$  mmHg,  $P < 0.01$ ) underwent acute open chest electrophysiologic and pathologic studies. We measured refractoriness at the atrial appendages at 3 cycle lengths (CL); conduction velocities at Bachmann's bundle, both atrial appendages and free walls at 4 CLs; conduction heterogeneity; atrial wavelength and AF duration. We performed light microscopy (LM) and electron microscopy (EM) and collagen and apoptosis studies. EBP was associated with widespread conduction abnormalities, shortening of atrial wavelength, and increased AF. There was no significant change in refractoriness. LM demonstrated atrial myocyte hypertrophy and myolysis in all EBP sheep and focal scarring in six. EM demonstrated mitochondrial and nuclear enlargement and increased collagen fibrils in EBP sheep, findings not present in any controls. Atrial collagen and apoptosis were increased in EBP animals.

**Conclusion** This study demonstrates that chronically, EBP is associated with significant atrial electrical and structural remodelling. These changes may explain the increased propensity to atrial arrhythmias observed with long-standing EBP.

## Introduction

Hypertension affects one billion people worldwide and is the most common treatable cause of AF. A continuum of risk exists between systolic and diastolic blood pressure and cardiovascular disease outcomes.<sup>1</sup> However, despite the importance of the association between AF and elevated blood pressure (EBP), there is a relative paucity of data describing the atrial remodelling that occurs as a result of chronically EBP. Long-standing BP elevation results in left ventricular hypertrophy, diastolic dysfunction, and as a result left atrial enlargement. Chronic atrial stretch may lead to abnormalities in atrial electrophysiology and pathology, but to date, these changes are poorly described.

We studied the effects of EBP in a chronic ovine model.<sup>2,3</sup> Pregnant ewes exposed to corticosteroid for 48 h in the first trimester of gestation produce offspring with hypertension

from the first few months of life, which is more marked in males and progresses with age. Previously described cardiovascular consequences of EBP in this model include increased left ventricular mass, impaired cardiac fractional reserve, and an increase in ventricular type 1 collagen.<sup>4</sup>

The aim of the present study was to characterize the pattern of atrial remodelling seen with chronically EBP of 4–5 years duration in this model. We performed detailed electrical and structural studies to describe these changes.

## Methods

The study was approved by the University of Melbourne Animal Experimentation Ethics Committee. Male sheep ( $55 \pm 8$  kg) subjected to prenatal corticosteroid (EBP) or saline (control) exposure were studied. Only singleton male foetuses were used in the study with a randomized allocation to corticosteroid or saline. The number of singleton male offspring born were nine in the saline group and 13 in the corticosteroid group. Two animals in the saline and one animal in the corticosteroid group died before the animals were studied at the age of 4.4 years. To maintain

\* Corresponding author. Tel: +61 3 93495400; fax: +61 3 93495411.  
E-mail address: jon.kalman@mh.org.au

an equal number of animals in each group, one saline-exposed animal was randomly not included. This animal model has previously been extensively described.<sup>2-4</sup> In brief, pregnant ewes received intravenous corticosteroid at 27 days' gestation. The cohort exposed to *in utero* corticosteroid developed significant elevation in blood pressure from 3 to 4 months, which increased with ageing.

Twelve EBP sheep (mean age of  $4.5 \pm 0.5$  years, systolic BP  $112 \pm 8$  mmHg, and diastolic BP  $85 \pm 11$  mmHg) and six control sheep ( $4.4 \pm 0.7$  years, systolic BP  $89 \pm 6$  mmHg, diastolic BP  $61 \pm 13$  mmHg,  $P < 0.0001$  for systolic and diastolic BP) were studied. General anaesthesia was induced with thiopentone to facilitate endotracheal intubation and then maintained with isoflurane 1.5%. Continuous monitoring of BP, heart rate, central venous pressure, end tidal CO<sub>2</sub>, and temperature was performed. Serial arterial blood gases were adjusted to maintain physiologic levels, and serum potassium was maintained between 4.5–5 mmol/L.

Intracardiac echocardiography (ICE) was performed in eight EBP sheep and four control sheep selected at random from each group. Under general anaesthesia, prior to open thoracotomy, the ICE catheter (Acunav, Acuson Computed Sonography) was introduced via the internal jugular vein. A mean of 5 cardiac cycles were averaged for each measurement.

A left thoracotomy was then performed, the heart exposed, and a pericardial cradle created. Custom designed epicardial plaques containing silver plated copper electrodes were sutured to the RAA and LAA, RAFW and LAFW, and BB. The plaque ( $72 \times 48$  mm) spanning Bachmann's bundle was sutured to the base of the RAA and was positioned anterior to the aorta, with the electrodes enface to the atrium as it traverses from right to left. The opposite end of the plaque was sutured to the base of the LAA. The detailed configuration of these plaques is shown in Figure 1. A total of 640 electrodes with an interelectrode distance of 2.4–2.5 mm together with a surface ECG were attached to a computerized mapping system (Unemap, Uniservices) which incorporated bipolar pacing and bipolar stored electrograms for offline analysis. Bipolar electrograms were created as the difference between pairs of electrodes with an overlapping configuration (e.g. bipolar electrogram A1 is

the electrode pair of A1 and B1). As a result, a 128 electrode plaque provides 117 bipolar electrograms, as the last electrode of the row has no pair and thus does not exist as a bipole.

## Electrophysiology study

### Atrial ERP

Atrial ERP was measured from four sites: two at the RAA and two at the LAA. Atrial ERP was measured at twice diastolic threshold (for a pacing threshold of  $<2$  mA) at cycle lengths (CL) of 500, 350, and 200 ms. At each site, the ERP was measured three times during each CL, and if the maximum and minimum amounts differed by  $>10$  ms, two additional measurements were taken and the total averaged. Rate adaptation was calculated as the difference between AERP<sub>500</sub> and AERP<sub>200</sub>.

### Atrial conduction

#### S1 conduction

Conduction was measured during stable bipolar atrial pacing (S1) at CLs of 500, 400, 300, and 200 ms from the following six atrial sites: RAA, RAFW, LAA, LAFW, right side BB, and left side BB (Figure 1). Pacing was performed from an electrode pair at one end of the BB plaque and conduction assessed at the opposite end. The process was repeated in the reverse direction. Pacing was also performed from bipolar pairs at two corners of the triangular plaques at the RAA, LAA, and RAFW. Pre-specified corners of the triangular plaque were utilized for pacing to ensure conduction was assessed in similar directions in each animal.<sup>5</sup> Conduction at the LAFW was evaluated during pacing from the LAA.

Isochronal maps of the atria were then created at 3 ms intervals in local activation time to assess conduction. Conduction velocity was measured through the sector of least isochronal crowding, as this was considered most likely to represent the direction of impulse propagation. Conduction was also assessed away from the plaque edges. In particular, CV was measured perpendicular to consecutive isochrones in the direction of the activation front between two

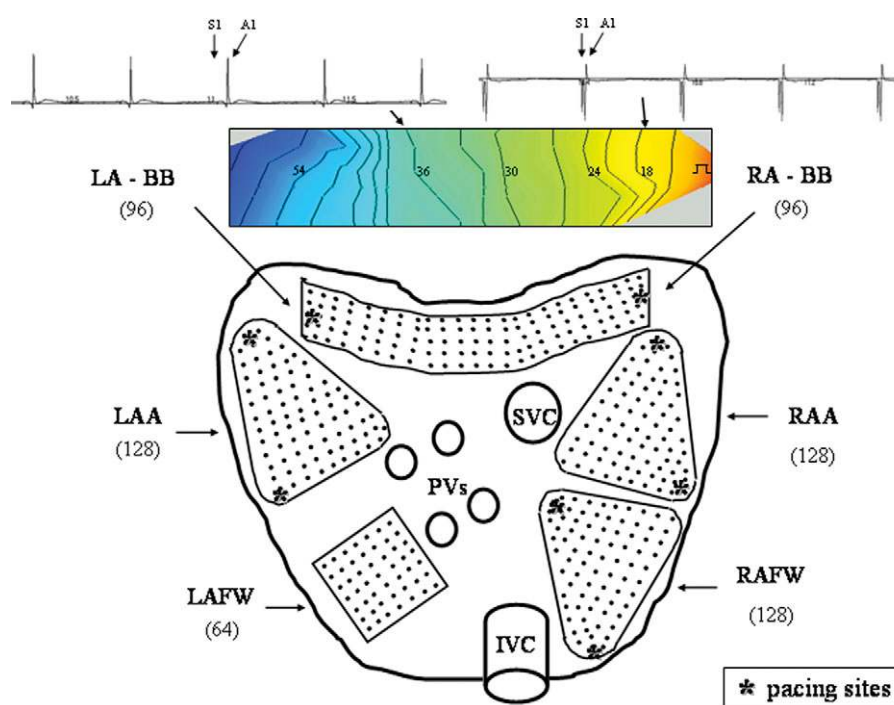


**Figure 1** Epicardial plaques were positioned on the RAA, LAA, RAFW, LAFW, and BB. The number of electrodes on each plaque is presented in brackets. A representative example of an isochronal map and electrograms from the plaque positioned across Bachmann's bundle is demonstrated during pacing from the right atrial end.

pairs of points three to four electrodes apart. A constant activation time between was required for this region to be utilized in determining CV. Activation maps were reviewed to ensure continuous longitudinal propagation, and only data with correlation coefficients  $>0.90$  were accepted.<sup>6</sup> Conduction times (CT) were measured between two pairs of points three electrodes apart. As with CV, the CT at each site was determined as the mean of the CT over five consecutive beats, following 15 s of stable capture.

#### Functional conduction delay

During programmed extra-stimulus testing from the RAA and LAA (BCL 350 ms), atrial conduction was also evaluated from the shortest S2 with a propagated response. The CT and CV during S2 was averaged from conduction measured across the plaque in each of five equal sectors once again applying the same methodology as described earlier.

#### Heterogeneity in conduction slowing

To assess the effects of prematurity on inhomogeneity in conduction, activation across the plaque was assessed during programmed extrastimulus testing following the shortest S2 with a propagated response at a BCL of 350 ms. The local CT (ms) was calculated from the maximum difference in the activation time of each quadruplet of bipoles. Local CV was then calculated by dividing the difference in the activation time by the interelectrode distance (mm). The local CVs were then plotted on a grid, as demonstrated in Figure 2A.<sup>7</sup> Slow conduction was defined as a local CV between 10 and 20 cm/s and conduction block as a CV of  $\leq 10$  cm/s.<sup>7</sup> Regions of conduction slowing or block were then displayed on a grid to demonstrate the spatial heterogeneity in conduction and calculate the percentage of the plaque occupied by conduction delay. The detailed methodology used is summarized in Figure 2A. Because of the triangular shape of the plaque, several bipoles along the edge were in groups of three rather than four and therefore contributed half of a square. An area of  $5 \times 5$  mm around the pacing site was typically excluded from analysis owing to pacing stimulus artefact obscuring the atrial electrogram.

#### Atrial wavelength

The wavelength for re-entry was calculated as the product of atrial ERP and CV at the RAA and LAA.

#### P-wave duration

P-wave duration was measured from lead II on the surface ECG as an average of 10 consecutive beats.

#### Sinus node function

The maximum corrected sinus node recovery time (CSNRT) was assessed following pacing at CLs of 500, 350, and 200 ms following a 30 s pacing train.

#### AF inducibility

A rigid protocol was observed for AF induction involving rapid atrial pacing at the RAA. Pacing was initiated at a CL of 200 ms and decreased in 5 ms intervals until either AF was initiated or Wenckebach atrial capture was reached. At Wenckebach threshold, pacing was maintained for 10 s. Induction was repeated 10 times. AF was considered to be induced if a rapid irregular atrial rhythm persisted  $>1$  s.<sup>8</sup> To estimate mean AF duration, AF was induced 10 times for AF duration  $<10$  min and five times for AF duration between 10 and 30 min. Electrical cardioversion was performed if AF persisted at least 30 min or resulted in significant hypotension. The maximum duration of AF was calculated as the longest episode of AF during the induction protocol.<sup>9</sup>

#### Pathology

At the completion of electrophysiologic evaluation, the animal was euthanized and the heart rapidly harvested for pathological studies.

At autopsy, the atria were dissected from the ventricles and gross epicardial fat was removed.

#### Atrial collagen

##### Total collagen content and concentration

The collagen content in the left and right atria from control and EBP sheep was determined by hydroxyproline analysis of tissue samples.<sup>10</sup> Duplicate 10  $\mu$ L aliquots from each sample were analysed for hydroxyproline content, using a scaled-down version of the procedure by Bergman and Loxley.<sup>11</sup> Hydroxyproline values were then converted to collagen content by multiplying by a factor of 7.46, whereas collagen concentration was derived by dividing collagen content by the dry weight tissue.

##### Collagen subtypes

The insoluble interstitial matrix collagens (I, III, V) were extracted from 2% of the total wet weight tissue from each control and EBP sheep atria.<sup>10</sup> The maturely cross-linked collagen was extracted by limited pepsin digestion (enzyme:substrate ratio, 1:10) for 24 h at 4°C, before aliquots of each sample, analysed by SDS-PAGE. Samples were run on 5% (wt./vol.) acrylamide gels containing 3.5% (wt./vol.) stacking gels.<sup>10</sup> Interrupted electrophoresis with delayed reduction of the disulphide bonds of type III collagen was used to separate the  $\alpha 1(\text{III})$  chains from the  $\alpha 1(\text{I})$  collagen chains.<sup>12</sup> The gels were stained overnight at 4°C with 0.1% (wt./vol.) coomassie brilliant blue R-250 and destained with 30% (vol./vol.) methanol containing 7% (vol./vol.) acetic acid, before being dried and photographed. Densitometry of the type I and III collagen chains was performed using a Bio-Rad GS-710 Calibrated Imaging Densitometer (Richmond, CA, USA) and Quantity-One software (Bio-Rad), and the ratio of type I to III collagen extrapolated in each group.

#### Histology

##### Light microscopy

Specimens from the RAA, LAA, and interatrial septum were uniformly harvested from each sheep and fixed by immersion in 10% neutral buffered formalin for histological examination. Standard techniques were used for dehydration in graded ethanol, clearance in xylene, and paraffin embedding of all specimens. Serial 2  $\mu$ m thick paraffin-embedded sections of each specimen were stained with haematoxylin and eosin (HE), Masson's trichrome, toluidine blue, periodic acid Schiff (PAS) and Congo red. Myofibrillar distribution was evaluated only in those myofibres in which a nucleus was identifiable in the plane of section.<sup>13</sup> Myofibrillar loss was semi-quantitated as mild ( $<10\%$  of the sarcoplasm devoid of myofibrils), moderate (10–25%), or severe ( $>25\%$ ).

##### Electron microscopy

Following light microscopy (LM) examination, representative specimens were selected from six EBP and four control sheep. Ultrathin sections of 80 nm thickness were cut from selected blocks, mounted on copper grids, stained with 2% uranyl acetate and lead citrate, and examined with a Siemens 102 electron microscope at 60 kV.

#### Apoptotic markers

Total protein from right and left atrial tissues of four control and seven EBP sheep was extracted using Trizol reagent and quantified using the BioRad Protein-Dye reagent assay. Equal aliquots of the sheep atrial extracts, containing 100  $\mu$ g of total protein were then electrophoresed on 10.5% acrylamide gels. The gel contents were electroblotted onto PVDF membranes, blocked in 5% skim milk powder, and then incubated with monoclonal IgG primary antibodies to either Bcl-2 or Caspase-3, overnight at room temperature. Membranes were then washed and treated with a goat anti-mouse IgG secondary antibody (1:2500 dilution).

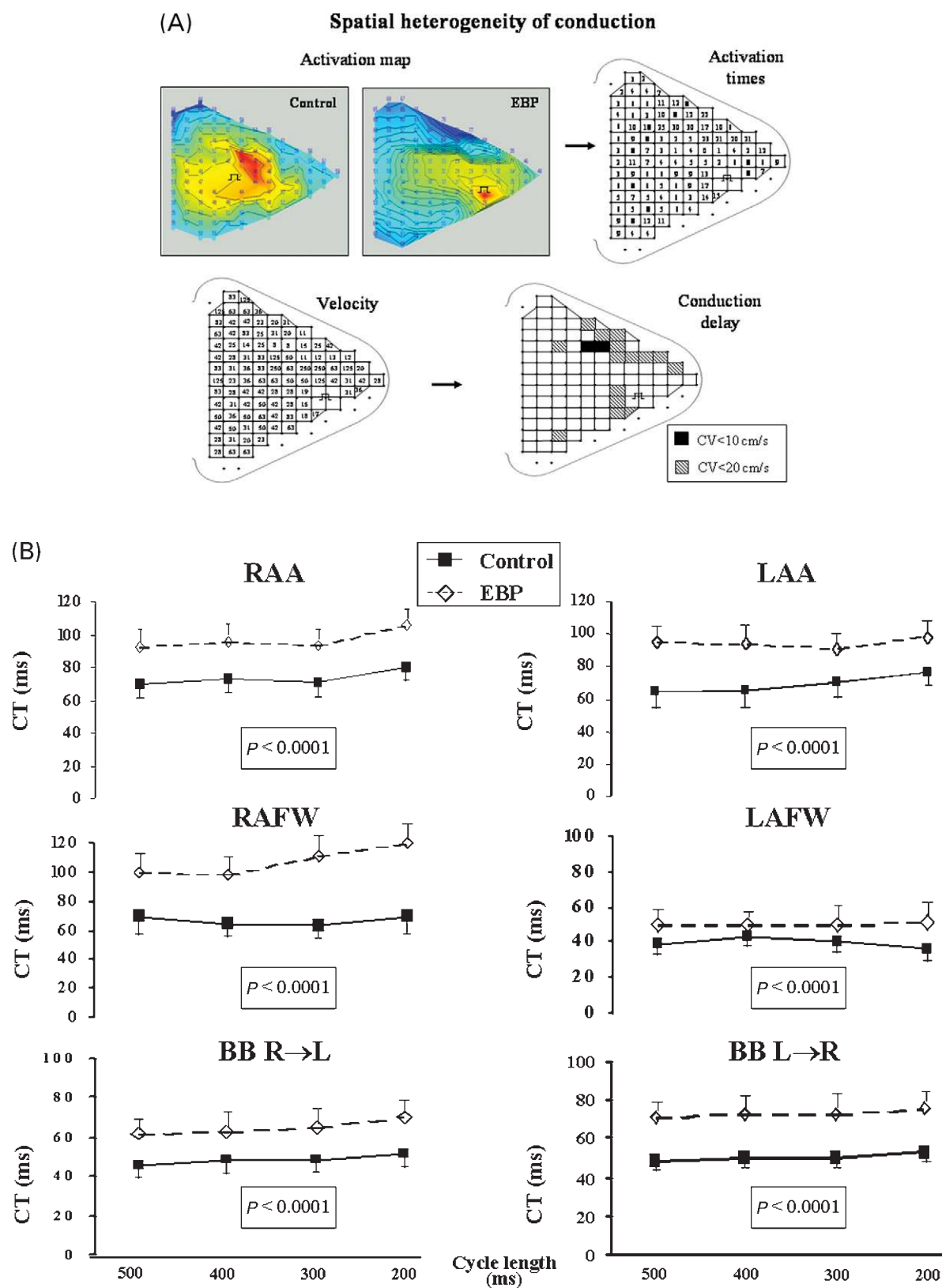


**Figure 2** (A) Spatial heterogeneity of conduction was assessed during the last propagated atrial response before refractoriness. Conduction was quantified by the local activation times calculated from four neighbouring bipoles ( $2.5 \times 2.5$  mm) in the direction of the conduction vector. Regions of conduction slowing and block were plotted to estimate the percent region of slow conduction. The initial map is from a control animal in which conduction slowing involved 3% of the total plaque area compared with an EBP animal in which conduction slowing involved 16.7% of the total plaque area. (B) CT were universally prolonged in the EBP group. (C) Conduction velocities were universally reduced in the EBP group.

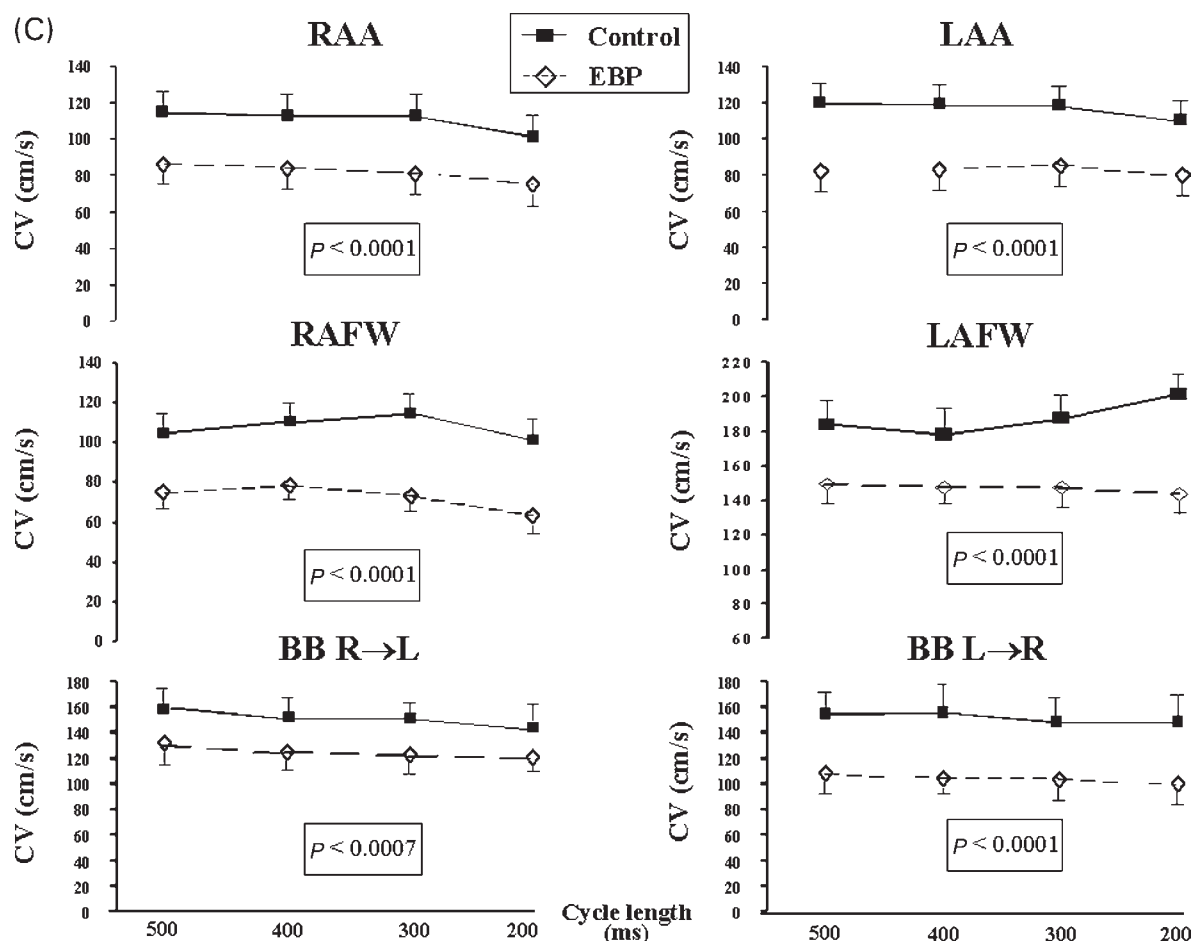


Figure 2 Continued.

The membranes were washed again and incubated with enhanced chemiluminescence reagent before being exposed to X-ray film and photographed. The X-ray films were also analysed by the densitometry of the Bcl-2 (25 kDa) or Caspase-3 (32 kDa) bands, as described previously.

### Statistical analysis

Data are expressed as mean  $\pm$  SD. Sample size was determined by previous studies.<sup>8</sup> A two-sided *t*-test was used only when single comparisons between groups were performed. These included AF inducibility, sinus node recovery time, and P-wave duration. All other comparisons were performed by repeated measures ANOVA, with *post hoc* analysis using the Newman-Keuls procedure. Comparisons were made between the EBP and control animals for each site and CL. Correlations were not made within an animal between the different sites and CLs. Proportions were compared by Fisher's exact test. Statistical significance was assumed at  $P < 0.05$ .

## Results

### Baseline characteristics

Twelve EBP sheep and six control sheep completed the study. There was a significant difference in systolic, diastolic, and arterial blood pressure between the two groups, with remaining baseline parameters well matched. Animal characteristics are presented in Table 1 from the day of study prior to open thoracotomy.

Table 1 Animal characteristics

	EBP (n = 12)	Control (n = 6)	P-value
Systolic BP (mmHg)	112 $\pm$ 12	89 $\pm$ 6	<0.0001
Diastolic BP (mmHg)	85 $\pm$ 11	61 $\pm$ 13	<0.0001
Mean arterial pressure (mmHg)	94 $\pm$ 3	70.7 $\pm$ 3.6	<0.0001
CVP (mmHg)	5.8 $\pm$ 1.7	5.2 $\pm$ 3.2	NS
Left atrium AP diameter (mm)	43 $\pm$ 2	39 $\pm$ 3	0.04
Left Ventricle LVDd (mm)	42 $\pm$ 5	38 $\pm$ 7	NS
LVDs (mm)	27 $\pm$ 4	27 $\pm$ 4	NS
PW thickness (mm)	11.8 $\pm$ 1	8.8 $\pm$ 0.1	<0.0001
IVS thickness (mm)	12.0 $\pm$ 0.7	10.3 $\pm$ 0.8	0.02
LV mass (g)	181 $\pm$ 32	127.5 $\pm$ 4	0.01

CVP, central venous pressure; AP, anteroposterior; LVDd, left ventricular diameter in diastole; LVDs, left ventricular diameter in systole; PW, posterior wall; IVS, interventricular septum.

### Intracardiac echocardiography

The cardiac dimensions as assessed by ICE are presented in Table 1. The EBP group demonstrated larger left atrial dimensions, an increase in interventricular septal and posterior wall thickness. Left ventricular mass was also significantly increased in the EBP group.

## Atrial refractoriness

Data for all measures of atrial refractoriness are presented in Table 2. There was no significant difference in the atrial ERP between the EBP group and controls at all atrial sites and CLs, and the rate adaptation of refractoriness was maintained (Table 2).

## Atrial conduction

### S1 conduction

At all sites and at all CLs, atrial conduction was reduced in the EBP group compared with controls. This achieved statistical significance for CT and velocity at all atrial sites (RAA, RAA, LAA, LAA) and CLs (Figure 2B and C). Conduction velocity across BB was significantly reduced in the EBP group at all CLs during pacing from the LA side and at 3 CLs when pacing from the RA side (Figure 2B). CT

across BB was significantly reduced in the EBP group at all CLs during pacing from both the LA side and RA sides (Figure 2C).

### Functional conduction velocity slowing

Conduction slowing was also observed in the EBP animals compared with controls with the shortest S2 interval that led to a propagated atrial response during ERP testing at the RAA and LAA (Figure 3). At the RAA S2, CT was  $13.1 \pm 2.5$  ms in the EBP compared with  $9.4 \pm 0.7$  ms in the controls ( $P=0.01$ ). At the LAA S2, CT was  $13.2 \pm 2.2$  ms in the EBP compared with  $10.2 \pm 1.6$  ms in the controls ( $P=0.02$ ). At the RAA S2, CV was  $62 \pm 9$  cm/s in the EBP compared with  $82 \pm 9$  cm/s in the controls ( $P=0.002$ ). At the LAA S2, CV was  $61 \pm 10$  cm/s in the EBP compared with  $74 \pm 10$  cm/s in the controls ( $P=0.02$ ).

### Heterogeneity of conduction

#### Spatial heterogeneity of conduction slowing

During the S1, drive train at 350 ms conduction slowing and block was not seen in either group. However, discrete regions of conduction slowing and block were increased during the shortest S2 interval, which led to a propagated atrial response in the EBP group (Figure 2A). At the LAA, local conduction delay was significantly increased to  $8.3 \pm 7.2\%$  of the plaque area in EBPs vs.  $1.6 \pm 1.1\%$  in controls ( $P=0.01$ ). At the RAA, local conduction delay was present in  $5.6 \pm 6.6\%$  of the plaque area in EBPs vs.  $2.1 \pm 3.3\%$  in controls ( $P=0.29$ ). At the LAA, conduction block was demonstrated in  $0.9 \pm 0.5\%$  of the plaque area in EBPs vs.  $0 \pm 0\%$  in controls ( $P=0.25$ ) and was not present in either group at the RAA.

### Atrial wavelength

Atrial wavelength was significantly shorter in the EBP group compared with controls at both the RAA and LAA (Table 2).

Parameter	EBP (ms)	Control (ms)	P-value
RAA ERP500	$149 \pm 22$	$154 \pm 39$	NS
RAA ERP350	$147 \pm 16$	$153 \pm 37$	NS
RAA ERP200	$139 \pm 14$	$147 \pm 21$	NS
LAA ERP500	$139 \pm 18$	$138 \pm 27$	NS
LAA ERP350	$140 \pm 20$	$137 \pm 26$	NS
LAA ERP200	$128 \pm 18$	$127 \pm 19$	NS
RAA ERP rate adaptation	$13 \pm 15$	$19 \pm 19$	NS
LAA ERP rate adaptation	$11 \pm 9$	$11 \pm 11$	NS
RAA WL500	$13 \pm 4$	$20 \pm 6$	0.01
RAA WL350	$12 \pm 2$	$19 \pm 4$	0.01
RAA WL200	$10 \pm 1$	$15 \pm 1$	0.002
LAA WL500	$12 \pm 2$	$17 \pm 5$	0.01
LAA WL350	$12 \pm 2$	$16 \pm 5$	0.04
LAA WL200	$11 \pm 2$	$14 \pm 3$	0.01

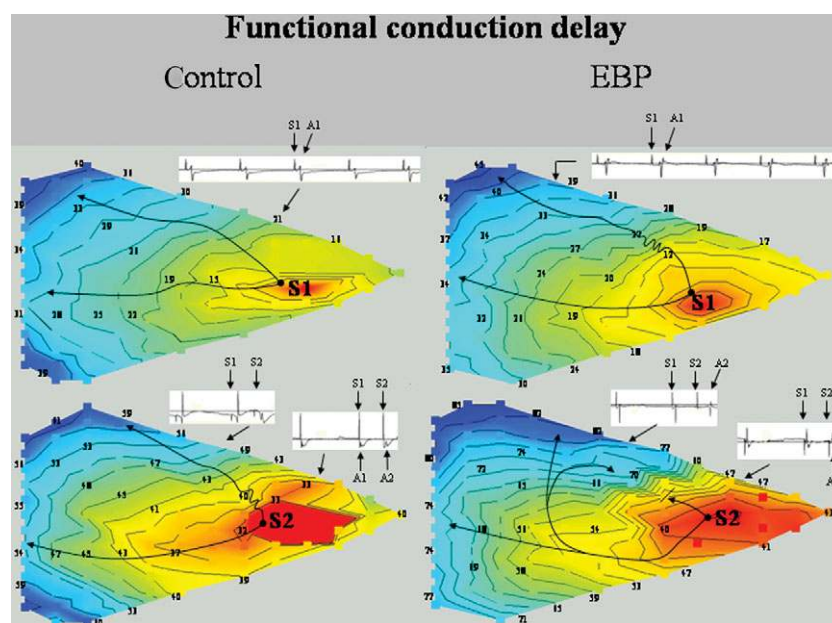


**Figure 3** S2 CVs were measured at right and LAAs. Representative examples demonstrate conduction slowing during both the S1 (top panel) and the shortest S2 with a propagated response (bottom panel) with discrete regions of conduction delay in EBP animals. In the top panels, representative electrograms during S1 drive are shown. In the bottom panels, representative electrograms from the last two beats of the S1 drive and the S2 are shown.

### P-wave duration

There was a significant increase in P-wave duration in EBP animals ( $52.4 \pm 5.4$  ms) compared with controls ( $44.3 \pm 4.5$  ms,  $P = 0.007$ ).

### Sinus node function

The CSNRT did not differ significantly between the two groups. The CSNRT at 500 ms was  $110 \pm 54$  in EBP animals vs.  $81 \pm 17$  ms in controls;  $135 \pm 22$  in EBP animals vs.  $160 \pm 45$  ms in controls at 350 ms; and  $156 \pm 63$  in EBP animals vs.  $130 \pm 96$  ms in controls at 200 ms ( $P$ , not significant).

### AF inducibility

The mean duration of the longest episode of AF was  $222 \pm 404$  s in the EBP group vs.  $2 \pm 3$  s,  $P = 0.005$ , in the control group. The mean duration of AF following 10 inductions was  $84 \pm 180$  s in the EBP group vs.  $0.5 \pm 1$  s,  $P = 0.002$ , in the control group. One animal in the EBP group required cardioversion after 4 min of AF because of associated hypotension which corrected following the restoration of sinus rhythm. All remaining animals reverted spontaneously (Figure 4).

### Atrial pathology

The total atrial weight was significantly increased in the EBP group ( $89 \pm 20$  g) compared with controls ( $62 \pm 14$  g;  $P = 0.01$ ). The total heart weight was  $316 \pm 84$  g in the EBP group vs.  $268 \pm 23$  g in the controls ( $P = 0.20$ ).

### Atrial collagen content and subtypes

Chronically, EBP was associated with a significant increase of 64% in total collagen content ( $P = 0.01$ ) and collagen concentration ( $P = 0.02$ ) in the ovine atria (Figure 5A).

Atrial tissues were predominantly composed of type I collagen monomers [ $\alpha 1(I)$  and  $\alpha 2(I)$  subunits] and dimers ( $\beta 11$ ,  $\beta 12$ ), whereas trace amounts of types III [ $\alpha 1(III)$  and  $\alpha 1(V)$  and  $\alpha 2(V)$ ] collagen monomers were also detected (Figure 5B). Densitometric analysis of these interstitial collagen chains demonstrated a significant increase in type I collagen with chronically EBP ( $P < 0.05$ ; Figure 5B), whereas no significant changes in types III and V collagen were detected. As a result, there was a trend towards an increased type I/III collagen ratio (by 30%,  $P = 0.13$ ).

### Histology

#### Light microscopy

In control sheep, myofibrils were uniformly and compactly distributed throughout the fibres (Figure 6A). In EBP sheep, there was mild-to-moderate perinuclear loss of myofibrils which extended a variable degree to the sarcolemma (Figure 6B). Myolysis was associated with myocyte hypertrophy, which was proportional to the magnitude of myofibrillar loss. In severe cases, the chamber wall thickness was appreciably increased. The nuclei of affected fibres were enlarged with the dispersion of chromatin and shallow invaginations of the nuclear membrane. Areas of myofibrillar loss appeared largely empty apart from a few small PAS-positive granules which corresponded to golden-brown pigment granules consistent with ceroid-lipofuscin in HE-stained sections.

There was a patchy increase in the interstitial space in the EBP group interspersed with regions where cellular ultrastructure was preserved. An increase in the number and size of fibroblasts was evident in the subendocardial connective tissue in EBP sheep, which were not present in control sheep. Discrete regions of chronic full-thickness

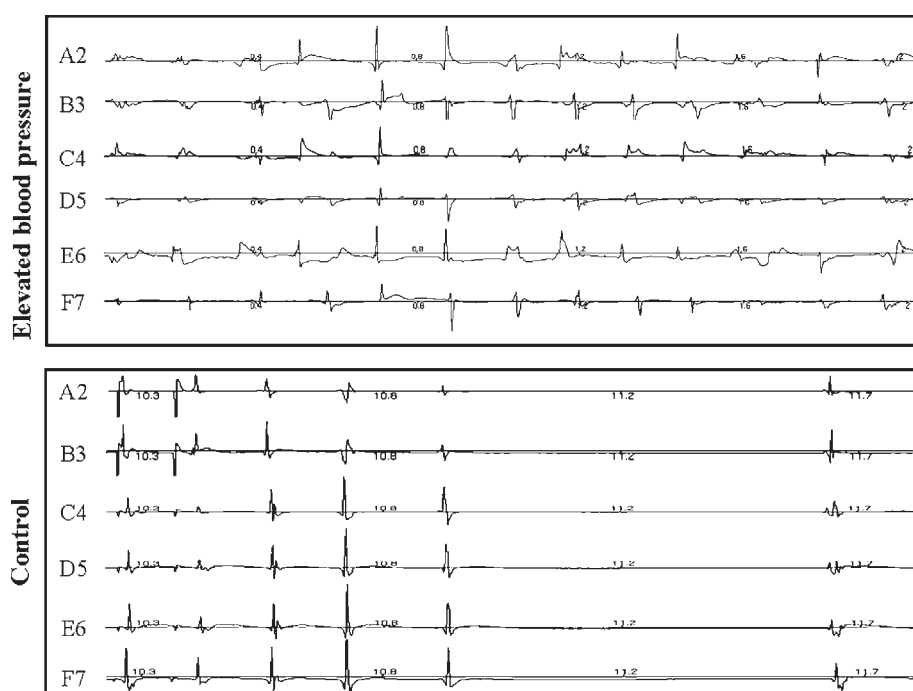


**Figure 4** Representative examples of simultaneous electrograms from six sites on the LAA plaque in response to rapid atrial pacing are demonstrated. AF was readily induced in EBP animals in contrast to controls in which only limited repetitive responses were seen.

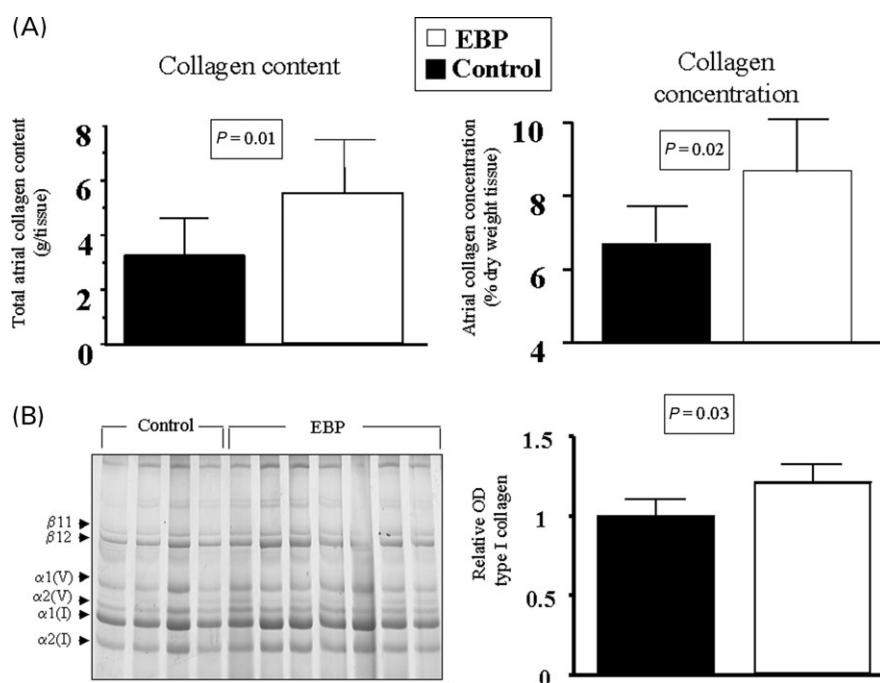


**Figure 5** (A) Atrial collagen content and concentration were increased in EBP animals. (B) Densitometric analysis of the insoluble interstitial collagens by SDS-PAGE demonstrated a significant increase in type I collagen in EBP animals, whereas no significant changes in types III and V collagen were detected (data not shown).

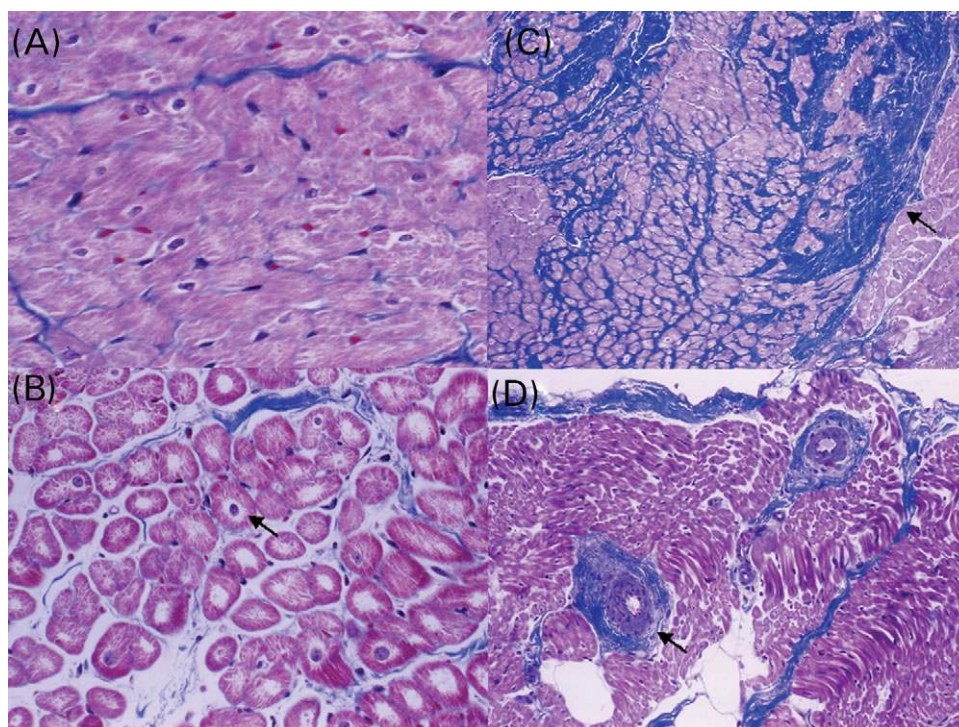


**Figure 6** (A) Masson's trichrome stain: transverse section of cardiac myofibrils demonstrating uniform staining of myofibrils across the sarcoplasm of each fibre in a control animal ( $\times 200$ ). (B) Loss of myofibrils from the perinuclear sarcoplasm in an EBP animal ( $\times 200$ ). (C) Patchy fibrosis and scarring were seen in six of 12 EBP animals ( $\times 50$ ). (D) Coronary arteriole demonstrating smooth muscle hypertrophy in the tunica media and marked concentric perivascular collagen in an EBP animal ( $\times 50$ ).

myocardial fibrosis or scarring were identified in six of 12 EBP sheep and in no controls (Figure 6C). Small-to-medium calibre coronary arteries in four of 12 EBP sheep showed mild-to-moderate smooth muscle hypertrophy of the tunica

media, with a variable excess of concentric perivascular collagen consistent with hypertensive change (Figure 6D). There was no evidence of inflammation, amyloid, or necrosis in either group.

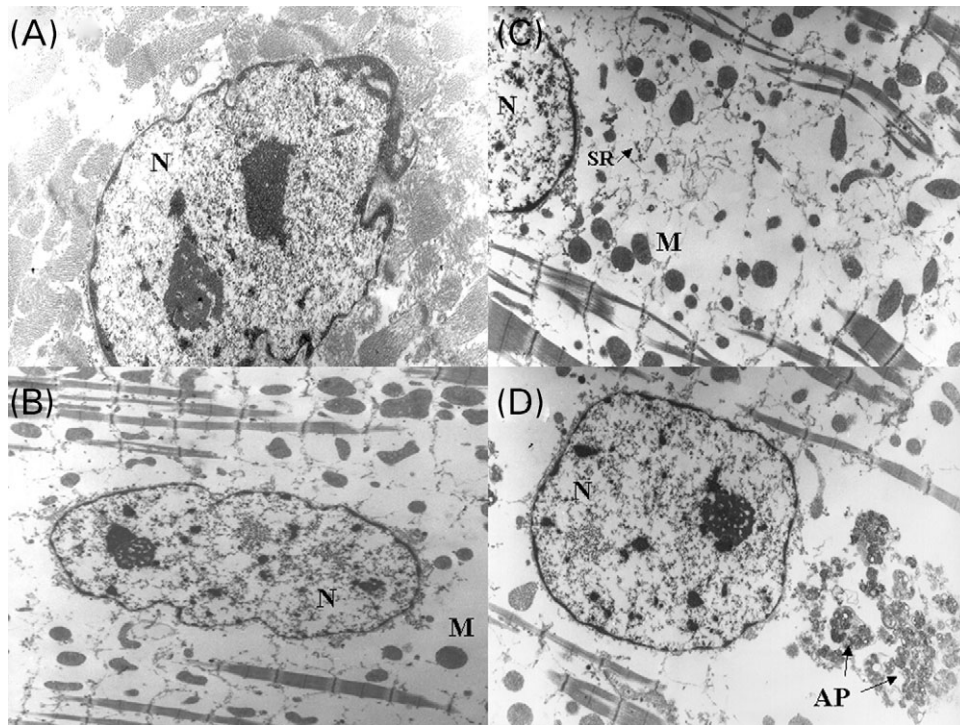


**Figure 7** (A) EM of atrial cardiac myofibre from a control sheep ( $\times 12\,500$ ). Sarcomeres closely abut the nucleus (N), with submembranous clumping of nuclear heterochromatin. (B) There is loss of sarcomeres from the perinuclear zone, with fragmentation of Z-lines apparent in adjacent residual sarcomeres in an EBP sheep. Enlarged mitochondria (M) are also seen ( $\times 12\,500$ ). (C) Fibrillary debris arising from disintegration of sarcomeres, enlarged mitochondria, and remnants of rough sarcoplasmic reticulum (SR) are seen in an EBP animal ( $\times 12\,500$ ). (D) Autophagosomes (AP) are demonstrated in the cytoplasm of an EBP sheep ( $\times 12\,500$ ).

### Electron microscopy

Transmission electron microscopy (EM) demonstrated mild-to-severe loss of myofibrils in the perinuclear sarcoplasm in EBP sheep (Figure 7B). In contrast, sarcomeres were uniformly distributed throughout the sarcoplasm and closely abutted the nucleus in myofibres from control sheep (Figure 7A). EBP was associated with fragmented myofilaments of residual sarcomeres at the periphery of the perinuclear zone of myofibrillary loss. Fragmentation was most obvious at the Z-lines, with the debris accumulating as fibrillary material in the perinuclear zone (Figure 7B). Intercalated discs were intact in both groups. Nuclei in EBP sheep typically displayed a more homogeneous distribution of chromatin, with small clumps of chromatin scattered randomly throughout without significant submembranous heterochromatin accumulation (Figure 7B). Mitochondria appeared mildly enlarged in myofibres from EBP sheep and often persisted in areas of sarcomere loss, together with remnants of rough sarcoplasmic reticulum (Figure 7C). Occasional myofibres from EBP sheep included perinuclear autophagosomes containing membranous structures and vacuoles (Figure 7D), and some myofibres contained dilated profiles of sarcoplasmic reticulum. Increased numbers of intercellular collagen fibrils were also apparent in the atria of EBP sheep.

### Atrial apoptosis

Apoptosis was upregulated in both atria in the EBP group. In the RA, caspase-3 was significantly increased in the EBP group ( $273 \pm 57$  AU) compared with controls ( $138 \pm 97$  AU,

$P = 0.01$ ), and Bcl-2 was significantly reduced in the EBP group ( $36 \pm 6$  AU) vs. controls ( $60 \pm 18$  AU,  $P = 0.01$ ). Similarly, in the LA, caspase-3 was significantly increased (EBP group  $79 \pm 12$  AU vs. controls  $54 \pm 10$  AU,  $P = 0.006$ ) and Bcl-2 was significantly reduced (EBP group  $40 \pm 16$  AU vs. controls  $64 \pm 17$  AU,  $P = 0.049$ ) with EBP.

### Discussion

This study presents detailed prospective information on the atrial electrophysiologic and structural changes associated with chronically EBP secondary to prenatal corticosteroid exposure. The following findings were observed in this model of chronically EBP:

- (i) Conduction slowing was demonstrated at all atrial sites and CLs together with an increase in the heterogeneity of conduction. Atrial wavelength was shortened in both atria.
- (ii) There was no significant difference in atrial refractoriness. Rate adaptation of refractoriness was maintained.
- (iii) These electrophysiologic abnormalities were associated with an increase in the duration of induced AF.
- (iv) Underlying the slowed conduction and tendency to AF, we observed significant structural changes. Atrial hypertrophy together with histologic changes characterized by central myofibrillolysis, myocyte hypertrophy, mitochondrial and nuclear enlargement, and increased intercellular collagen fibrils was demonstrated.
- (v) An increase in total atrial collagen predominantly due to an increase in type I collagen. Discrete full-thickness

subendocardial scarring was present in six of 12 EBP sheep and was not seen in any controls.

- (vi) An increase in atrial apoptosis as determined by an increase in the proapoptotic marker caspase-3 and a reduction in the antiapoptotic marker Bcl-2.

### Relationship between EBP and atrial fibrillation

EBP is the most prevalent and potentially treatable risk factor for AF. The range of pathophysiologic responses to EBP includes left hypertrophy, diastolic dysfunction, elevated left atrial pressure, and as a result, left atrial enlargement. Indeed, the magnitude of LA enlargement may be proportional to the degree of BP elevation.<sup>14</sup> In the Framingham study, the risk of developing AF increased by 39% for each 5 mm increase in left atrial size.<sup>14</sup> Blood pressure medication has been shown to resolve the structural changes of left atrial enlargement and left ventricular hypertrophy.

### Ovine model of chronically EBP

Arterial hypertension is a complex cardiovascular disorder which should be based not only on the absolute blood pressure level, but also on the recognition of end-organ damage and other cardiovascular risk factors. The pathogenesis of hypertension in humans remains incompletely understood and appears to be multifactorial. As in human hypertension, the cardiac sequelae in the current ovine model may not be determined by elevated pressure alone, but may also result from the underlying pathophysiologic mechanism.

The chronic ovine model of EBP used in the present study has previously been extensively characterized.<sup>2–4</sup> Epidemiological studies have established a link between reduced growth *in utero* and the subsequent development of hypertension and increased left ventricular mass.<sup>15</sup> A sub-optimal intrauterine environment is thought to permanently 'programme' fetal organs, facilitating survival in the short term but with adverse consequences in the long term.<sup>3</sup> Several animal models have created cardiovascular disease in the offspring by different interventions including maternal malnutrition, maternal anaemia, and exposure to increased glucocorticoid.<sup>2,16</sup> Notably in some of these cases, there is no evidence of reduced fetal growth.<sup>2</sup> The common factor in the long-term programming of the fetus appears to be increased levels of glucocorticoid. Dodic *et al.*<sup>2</sup> developed a unique model in which the pregnant ewe was exposed to corticosteroids for a critical period of 2 days at days 26–28 of gestation, resulting in offspring that had EBP. The animals develop BP elevation by the age of 4 months, which is chronic and progressive and plateaus beyond the age of 40 months.

The pathophysiologic mechanism responsible for EBP in adult offspring appears to involve the renin–angiotensin system. Upregulation of angiotensinogen and angiotensin type 1 receptors in the kidney and brain without change in the circulating levels of the renin–angiotensin system has been demonstrated in this ovine model.<sup>3</sup> In pregnant rats fed, a low protein diet hypertension in the offspring could be prevented by postnatal ACE-inhibition.<sup>17</sup> In a transgenic murine model of human angiotensinogen gene expression, blood pressure was elevated without an increase in peripheral angiotensin II.<sup>18</sup> Short-term peripheral

angiotensin receptor blockade did not reduce blood pressure in either murine or ovine models.<sup>19</sup> However, in a transgenic murine model of cerebral AT1 receptor overexpression, intracerebrovascular infusion of an angiotensin receptor blocker did reduce blood pressure.<sup>20</sup> Prior studies in the ovine model have not demonstrated a role for the hypothalamic pituitary adrenal axis<sup>2</sup> or testosterone in the genesis of EBP.<sup>3</sup> The level of BP elevation has been shown to lead to advanced cardiac sequelae including impaired cardiac fractional reserve, increased left ventricular mass, and increased left ventricular type 1 collagen in animals between 3 and 5 years of age.<sup>4</sup> In addition, in the present study, ICE demonstrated increased left ventricular wall thickness with associated left atrial enlargement. In order to characterize the atrial substrate that may be responsible for AF in chronically EBP, we studied such animals at a mean age of 4.5 years.

### Prior studies of atrial abnormalities in hypertension

Limited data are available regarding the changes in atrial electrophysiology in hypertension. In a retrospective study of patients with hypertension who subsequently developed AF, the independent predictors of AF were P-wave prolongation and increased P-wave dispersion.<sup>21</sup> To our knowledge, there are no prior studies detailing the nature of electrophysiologic remodelling occurring as a consequence of chronically EBP in animals or humans.

### Atrial remodelling

The concept of atrial electrical remodelling has been elegantly described by Wijffels *et al.*<sup>8</sup> as a shortening of ERP with loss of rate adaptation in response to even brief episodes of AF. The fall in ERP resulted in shortening of the atrial wavelength and the observation that 'AF begets AF'. In a range of conditions associated with AF, atrial structural change and, in particular, atrial fibrosis and its consequences for atrial conduction slowing and heterogeneity have been described.<sup>9,22,23</sup> In the canine heart failure model, Nattel and coworkers<sup>22</sup> demonstrated no change in atrial ERP but an increase in conduction heterogeneity and an increase in AF duration. Discrete regions of slow conduction were associated with histologic evidence of extensive interstitial fibrosis. Importantly, a follow-up study demonstrated that with reversal of heart failure, there is complete recovery of ionic remodelling, but the AF substrate and structural remodelling remained.<sup>24</sup> This suggested that structural, rather than ionic, remodelling may be the primary contributor to chronic AF maintenance. In support of this, human studies of atrial remodelling in heart failure have similarly shown the primary AF substrate to be conduction slowing with indirect evidence of atrial fibrosis.<sup>25</sup> Of note, the nature of atrial remodelling seen in the canine model of heart failure bears some striking similarities to that observed in the current study of EBP. In the present study, animals with EBP for several years demonstrated widespread conduction slowing with no change in atrial refractoriness. These electrophysiologic consequences of long-standing EBP were associated with both an increase in total atrial collagen and atrial weight. Indeed, not only was conduction slowed, but there was also an increase in spatial heterogeneity of conduction slowing consistent with the patchy nature of fibrosis observed. Such

abnormalities are well recognized to provide the substrate for multiple wavelet re-entry and were associated with increased AF in this model.

Other pathophysiologic conditions which cause atrial stretch and AF, such as mitral regurgitation,<sup>9,23</sup> have also been shown to cause an increase in conduction heterogeneity and atrial fibrosis, raising the possibility that these differing processes—EBP, heart failure, mitral regurgitation—may have a final common pathway by which they lead to AF. However, whether stretch, the renin-angiotensin system, or other unidentified factor or a combination of factors is responsible for the observed changes remains unclear.

### Atrial ultrastructural remodelling

Atrial histologic changes have been demonstrated in response to both rapid atrial pacing and heart failure. Following 9–23 weeks of rapid atrial pacing, Ausma *et al.*<sup>13</sup> demonstrated loss of sarcomeres, cellular hypertrophy, and dispersion of nuclear chromatin with preservation of the interstitial space. In an elegant follow-up study, the resolution of structural remodelling was shown to be a 'slow process', incomplete 4 months, following the restoration of sinus rhythm.<sup>26</sup> In contrast, the atrial changes in heart failure were marked by extensive interstitial fibrosis.<sup>22</sup> Similar histologic appearances were present in the current study of chronically EBP, with cellular hypertrophy, perinuclear loss of sarcomeres, and a patchy increase in the interstitial space with areas of subendocardial fibrosis next to regions where the interstitial space was preserved. As in patients with lone AF, type I collagen was the predominant collagen subtype in EBP animals.<sup>27</sup> A 30% increase in the collagen type I:III ratio was also demonstrated implicating a role for mechanical stretch in the pathophysiologic mechanism of fibrosis in EBP animals.<sup>28</sup> Similar to both heart failure and rapid atrial pacing models, there was a distinct absence of inflammation or necrosis.

### Atrial apoptosis

Apoptosis is the process of programmed cell death, which is physiologic but also occurs in a range of pathologic conditions. In the present study, the new finding of an increase in apoptosis in the atria of chronically EBP is described. An increase in the pro-apoptotic protein caspase-3 and a reduction in the anti-apoptotic protein Bcl-2 are consistent with the findings of Aïme-Sempe *et al.*,<sup>29</sup> who reported apoptosis in the atria of patients with chronic AF and left ventricular dysfunction. Apoptosis has been extensively described in the ventricle in a range of cardiac conditions including hypertension.<sup>30,31</sup> Increased apoptosis has been demonstrated in animal models of renal hypertension, angiotensin II-induced hypertension, and spontaneously occurring hypertension.<sup>32</sup> Apoptosis has also been demonstrated in biopsy specimens from humans with left ventricular hypertrophy,<sup>30</sup> with a further increase seen in the decompensated hypertrophied ventricle.<sup>31</sup> Gonzalez *et al.*<sup>31</sup> suggested that humoral factors may be critical in stimulating apoptosis in hypertension on the basis of the observations that (i) apoptosis is not confined to the left ventricle,<sup>30,32</sup> (ii) antihypertensive therapy reduces apoptosis independent of effect on blood pressure,<sup>30,32</sup> and (iii) apoptosis has not been observed when left ventricular hypertrophy occurs in response to

aortic stenosis. In hypertensive patients randomized to treatment with either Losartan or Amlodipine, apoptosis in the ventricle was significantly reduced in the group receiving the angiotensin receptor blocker despite equivalent blood pressure reductions.<sup>30</sup> Together these findings suggest that humoral factors are important in the activation of apoptosis in hypertension. Although in the present study atrial apoptosis is described, more studies are required to define the underlying mechanism.

### Potential clinical implications

The findings in the present study have several potential clinical implications. The atrial substrate in EBP predominantly involves conduction slowing and an increase in the heterogeneity of conduction in association with atrial fibrosis. Angiotensin II is a potent promoter of atrial fibrosis leading to cardiac myoblast proliferation and reduction in collagenase activity but also stimulates atrial apoptosis. In a heart failure animal study, a reduction in atrial fibrosis and AF was demonstrated in the group treated with ACE-I compared with vasodilator therapy.<sup>33</sup> Retrospective studies in patients with left ventricular dysfunction have demonstrated a reduction in AF in the ACE-I group.<sup>34</sup> A recent retrospective study involving 10 000 hypertensive patients reported a reduction in AF in those treated with ACE-I compared with calcium channel blockers.<sup>35</sup> The increase in atrial collagen and apoptosis in the EBP group in association with conduction slowing and AF duration provide pathophysiologic insights into potential underlying mechanisms behind the recent clinical observations that medications which block the effects of angiotensin II may alter atrial substrate and reduce AF.

### Study limitations

The development of AF depends not only on the presence of atrial substrate but also importantly on the presence of triggers. It is possible that by producing atrial and pulmonary vein stretch, chronically EBP may play a role in the appearance of pulmonary vein triggers. In this ovine model, pulmonary vein muscular sleeves are sparse or absent and therefore an analysis of pulmonary vein electrophysiology could not be performed. We speculate that the angiotensin II system may be important in the pathophysiologic mechanism responsible for the observed changes. Therefore, the atrial expression of the angiotensin II system forms part of a recently commenced protocol examining the underlying pathophysiologic mechanisms and the effect of antihypertensive therapy in this model. Atrial electrophysiologic and structural data shortly after birth in future animal cohorts would be of interest to investigate the time course of the changes observed in the model.

### Conclusion

This study in a unique animal model demonstrates that chronically EBP, when present for 4–5 years, is associated with atrial remodelling characterized by the following electrical and structural changes: (i) widespread conduction slowing coupled with an increase in conduction heterogeneity; (ii) shortening of atrial wavelength; (iii) an increase

in atrial fibrosis and apoptosis; and (iv) cellular myolysis. In this study, these abnormalities led to an increase in AF duration. Similar abnormalities may in part be responsible for the increased propensity to atrial arrhythmias observed in patients with long-standing blood pressure elevation.

## Acknowledgements

P.M.K. is a recipient of a medical postgraduate research scholarship from the NHMRC of Australia. P.S. is a recipient of the Neil Hamilton Fairley and Ralph Reader Fellowship, jointly funded by the NHMRC and the NHF. This study was funded by a grant-in-aid from the NHF and the cardiovascular lipid (CVL) project.

**Conflict of interest:** none declared.

## References

- Vasan RS, Larson MG, Leip EP, Evans JC, O'Donnell CJ, Kannel WB, Levy D. Impact of high-normal blood pressure on the risk of cardiovascular disease. *N Engl J Med* 2001;**345**:1291–1297.
- Dodic M, May CN, Wintour EM, Coghlan JP. An early prenatal exposure to excess glucocorticoid leads to hypertensive offspring in sheep. *Clin Sci (Lond)* 1998;**94**:149–155.
- Dodic M, Abouantoun T, O'Connor A, Wintour EM, Moritz KM. Programming effects of short prenatal exposure to dexamethasone in sheep. *Hypertension* 2002;**40**:729–734.
- Dodic M, Samuel C, Moritz K, Wintour EM, Morgan J, Grigg L, Wong J. Impaired cardiac functional reserve and left ventricular hypertrophy in adult sheep after prenatal dexamethasone exposure. *Circ Res* 2001;**89**:623–629.
- Lammers WJ, Schalij MJ, Kirchhof CJ, Allesie MA. Quantification of spatial inhomogeneity in conduction and initiation of reentrant atrial arrhythmias. *Am J Physiol* 1990;**259**:H1254–H1263.
- Gaspo R, Bosch RF, Talajic M, Nattel S. Functional mechanisms underlying tachycardia-induced sustained atrial fibrillation in a chronic dog model. *Circulation* 1997;**96**:4027–4035.
- Eijsbouts SC, Majidi M, van Zandvoort M, Allesie MA. Effects of acute atrial dilation on heterogeneity in conduction in the isolated rabbit heart. *J Cardiovasc Electrophysiol* 2003;**14**:269–278.
- Wijffels MC, Kirchhof CJ, Dorland R, Allesie MA. Atrial fibrillation begets atrial fibrillation. A study in awake chronically instrumented goats. *Circulation* 1995;**92**:1954–1968.
- Verheule S, Wilson E, Everett T, Shanbhag S, Golden C, Olgin J. Alterations in atrial electrophysiology and tissue structure in a canine model of chronic atrial dilatation due to mitral regurgitation. *Circulation* 2003;**107**:2615–2622.
- Samuel CS, Butkus A, Coghlan JP, Bateman JF. The effect of relaxin on collagen metabolism in the nonpregnant rat pubic symphysis: the influence of estrogen and progesterone in regulating relaxin activity. *Endocrinology* 1996;**137**:3884–3890.
- Bergman I, Loxley R. New spectrophotometric method for the determination of proline in tissue hydrolyzates. *Anal Chem* 1970;**42**:702–706.
- Sykes B, Puddle B, Francis M, Smith R. The estimation of two collagens from human dermis by interrupted gel electrophoresis. *Biochem Biophys Res Commun* 1976;**72**:1472–1480.
- Ausma J, Wijffels M, Thone F, Wouters L, Allesie M, Borgers M. Structural changes of atrial myocardium due to sustained atrial fibrillation in the goat. *Circulation* 1997;**96**:3157–3163.
- Kannel WB, Wolf PA, Benjamin EJ, Levy D. Prevalence, incidence, prognosis, and predisposing conditions for atrial fibrillation: population-based estimates. *Am J Cardiol* 1998;**82**:2N–9N.
- Martyn CN, Barker DJ, Jespersen S, Greenwald S, Osmond C, Berry C. Growth in utero, adult blood pressure, and arterial compliance. *Br Heart J* 1995;**73**:116–121.
- Hoet JJ, Hanson MA. Intrauterine nutrition: its importance during critical periods for cardiovascular and endocrine development. *J Physiol* 1999;**514**:617–627.
- Sherman RC, Langley-Evans SC. Early administration of angiotensin-converting enzyme inhibitor captopril, prevents the development of hypertension programmed by intrauterine exposure to a maternal low-protein diet in the rat. *Clin Sci (Lond)* 1998;**94**:373–381.
- Morimoto S, Cassell MD, Beltz TG, Johnson AK, Davisson RL, Sigmund CD. Elevated blood pressure in transgenic mice with brain-specific expression of human angiotensinogen driven by the glial fibrillary acidic protein promoter. *Circ Res* 2001;**89**:365–372.
- Peers A, Campbell DJ, Wintour EM, Dodic M. The peripheral renin-angiotensin system is not involved in the hypertension of sheep exposed to prenatal dexamethasone. *Clin Exp Pharmacol Physiol* 2001;**28**:306–311.
- Lazartigues E, Dunlay SM, Lohli AK, Sinnayah P, Lang JA, Espelund JJ, Sigmund CD, Davisson RL. Brain-selective overexpression of angiotensin (AT1) receptors causes enhanced cardiovascular sensitivity in transgenic mice. *Circ Res* 2002;**90**:617–624.
- Ciaroni S, Cuenoud L, Bloch A. Clinical study to investigate the predictive parameters for the onset of atrial fibrillation in patients with essential hypertension. *Am Heart J* 2000;**139**:814–819.
- Li D, Fareh S, Leung TK, Nattel S. Promotion of atrial fibrillation by heart failure in dogs: atrial remodeling of a different sort. *Circulation* 1999;**100**:87–95.
- Verheule S, Wilson E, Banthia S, Everett TH, Shanbhag S, Sih HJ, Olgin J. Direction-dependent conduction abnormalities in a canine model of atrial fibrillation due to chronic atrial dilatation. *Am J Physiol Heart Circ Physiol* 2004;**287**:H634–H644.
- Cha TJ, Ehrlich JR, Zhang L, Shi YF, Tardif JC, Leung TK, Nattel S. Dissociation between ionic remodeling and ability to sustain atrial fibrillation during recovery from experimental congestive heart failure. *Circulation* 2004;**109**:412–418.
- Sanders P, Morton JB, Davidson NC, Spence SJ, Vohra JK, Sparks PB, Kalman JM. Electrical remodeling of the atria in congestive heart failure: electrophysiological and electroanatomic mapping in humans. *Circulation* 2003;**108**:1461–1468.
- Ausma J, van der Velden HM, Lenders MH, van Ankeren EP, Jongsma HJ, Ramaekers FC, Borgers M, Allesie MA. Reverse structural and gap-junctional remodeling after prolonged atrial fibrillation in the goat. *Circulation* 2003;**107**:2051–2058.
- Boldt A, Wetzel U, Lauschke J, Weigl J, Gummert J, Hindricks G, Kottkamp H, Dhein S. Fibrosis in left atrial tissue of patients with atrial fibrillation with and without underlying mitral valve disease. *Heart* 2004;**90**:400–405.
- Carver W, Nagpal ML, Nachtigal M, Borg TK, Terracio L. Collagen expression in mechanically stimulated cardiac fibroblasts. *Circ Res* 1991;**69**:116–122.
- Aime-Sempe C, Folliguet T, Rucker-Martin C, Krajewska M, Krajewska S, Heimbürger M, Aubier M, Mercadier JJ, Reed JC, Hatem SN. Myocardial cell death in fibrillating and dilated human right atria. *J Am Coll Cardiol* 1999;**34**:1577–1586.
- Gonzalez A, Lopez B, Ravassa S, Querejeta R, Larman M, Diez J, Fortuno MA. Stimulation of cardiac apoptosis in essential hypertension: potential role of angiotensin II. *Hypertension* 2002;**39**:75–80.
- Gonzalez A, Fortuno MA, Querejeta R, Ravassa S, Lopez B, Lopez N, Diez J. Cardiomyocyte apoptosis in hypertensive cardiomyopathy. *Cardiovasc Res* 2003;**59**:549–562.
- Diez J, Panizo A, Hernandez M, Vega F, Sola I, Fortuno MA, Pardo J. Cardiomyocyte apoptosis and cardiac angiotensin-converting enzyme in spontaneously hypertensive rats. *Hypertension* 1997;**30**:1029–1034.
- Li D, Shinagawa K, Pang L, Leung TK, Cardin S, Wang Z, Nattel S. Effects of angiotensin-converting enzyme inhibition on the development of the atrial fibrillation substrate in dogs with ventricular tachypacing-induced congestive heart failure. *Circulation* 2001;**104**:2608–2614.
- Vermes E, Tardif JC, Bourassa MG, Racine N, Levesque S, White M, Guerra PG, Ducharme A. Enalapril decreases the incidence of atrial fibrillation in patients with left ventricular dysfunction: insight from the Studies Of Left Ventricular Dysfunction (SOLVD) trials. *Circulation* 2003;**107**:2926–2931.
- L'Allier PL, Ducharme A, Keller PF, Yu H, Guertin MC, Tardif JC. Angiotensin-converting enzyme inhibition in hypertensive patients is associated with a reduction in the occurrence of atrial fibrillation. *J Am Coll Cardiol* 2004;**44**:159–164.